Hokkaido Mathematical Journal Vol. 43 (2014) p. 361–383

Ulam's cellular automaton and Rule 150

Akane Kawaharada

(Received August 30, 2012)

Abstract. In this paper we study Ulam's cellular automaton, a nonlinear almost equicontinuous two-dimensional cell-model of crystalline growths. We prove that Ulam's automaton contains a linear chaotic elementary cellular automaton (Rule 150) as a subsystem. We also study the application of the inverse ultradiscretization, a method for deriving partial differential equations from a given cellular automaton, to Ulam's automaton. It is shown that the partial differential equation obtained by the inverse ultradiscretization preserves the self-organizing pattern of Ulam's automaton.

Key words: Cellular automaton, symbolic dynamics, linear chaos, almost equicontinuity, inverse ultradiscretization, fractal pattern.

1. Introduction

A cellular automaton (CA) is a discrete dynamical system whose configurations are determined by a local rule acting on each cell in synchronous. Von Neumann and Ulam introduced it as a self-reproduction model in the early 1950s [23], [21]. A crucial property of CAs is that it can derive rich and complex behavior from simple rules. The macroscopic behavior of a CA often resembles that of natural phenomena, and therefore, CAs are used as models of complex systems in biology, physics, computer science and so on.

Mathematical studies of CAs have been developed after Hedlund's work where he studies CAs by means of symbolic dynamics [8]. Since then, there have been many results on topological properties of CAs [9], [13], [3].

Recently the relation between CAs and partial differential equations (PDEs) is focused [20], [11]. It is derived from Wolfram's question [25]; "What is the correspondence between CAs and differential equations?". It is important to consider the relation between continuous models and CA models, because in many cases natural phenomena are conventionally studied by continuous models such as PDEs. In this regard, there is a method called ultradiscretization to construct CAs directly from continuous equations [20]. Its inverse operation is called inverse ultradiscretization (IUD), which allows us to obtain a PDE associated with a CA.However the opera-

2010 Mathematics Subject Classification : 37B15, 37B10, 35Q92.

tion of IUD is not uniquely defined and therefore does not give the complete answer to Wolfram's question. It is not guaranteed that the obtained PDEs have the same or similar properties as the original CA's. It is not yet known how to describe the relation between a given CA and the corresponding PDEs in a mathematically rigorous manner.

In this paper, we will focus on two particularly important examples of CA; Ulam's CA and Rule 150. Ulam's CA is a simplified form of Ulam's cell-model [22] which creates fractal-like crystalline patterns (see Figure 5). The model can be regarded as a basis of Conway's game of life [14] by reason that for a particular initial configuration existing cells never dies during the time evolution of the model. Rule 150 is one of elementary CAs, which are one-dimensional CAs with possible two states $0, 1$ and their local rules defined by the nearest three neighborhood [24].

We show that a subsystem of Ulam's CA is topologically conjugate to the elementary CA called Rule 150. Ulam's CA is a nonlinear almost equicontinuous two-dimensional CA while Rule 150 is a linear chaotic one-dimensional CA. Our embedding of Rule 150 to Ulam's CA thus gives a new interesting dynamical phenomena where a linear chaos is contained in a nonlinear dynamical system [7]. We also study the application of IUD to Ulam's CA. It is shown that the PDE obtained by IUD preserve self-organizing patterns of Ulam's CA.

This paper is organized as follows. In Section 2 we give some definitions and notation. We also introduce the method of IUD. In Section 3 we introduce Ulam's CA and linear elementary CAs as typified by Rule 150. We show the relation between Ulam's CA and Rule 150. In Section 4 we perform IUD for Ulam's CA and Rule 150 and discuss the properties of the obtained PDE. Finally, Section 5 summarizes concluding remarks.

2. Preliminaries

Here we present definitions and notation on topological dynamical systems in Section 2.1, and on symbolic dynamics and CAs in Section 2.2. In Section 2.3 we introduce the method of IUD.

2.1. Topological dynamics

We define a *discrete dynamical system* by a pair (X, T) consisting of a compact metric space X with metric d and a continuous map $T : X \to X$. The n-th *iteration* of T is denoted by T^n, thus T^0 is the identity map on X.

Let (Y, S) be another dynamical system. Two topological dynamical systems (X, T) and (Y, S) are *topologically conjugate*, if there exists a *conjugacy* map, $\varphi : (X, T) \to (Y, S)$, which is a homeomorphism such that $\varphi \circ T = S \circ \varphi$. A set $A \subset X$ is *invariant* if $T(A) = A$. If A is invariant and closed, (A, T) is called a *subsystem* of (X, T).

A point $x \in X$ is a *periodic point* for T with period $n \geq 1$ if $T^n(x) = x$. In particular if $T(x) = x$, then x is called a *fixed point*. A point $x \in X$ is an *equicontinuous point*, if for any $\epsilon > 0$ there exists δ such that whenever $u \in X$ satisfies $d(x, u) < \delta$ then $d(T^n x, T^n u) < \epsilon$ for all $n > 0$. A point $x \in X$ is a *transitive point*, if it has a dense orbit in X.

We introduce some topological properties of dynamical systems.

Definition 1 Let (X, T) be a dynamical system.

1. A dynamical system (X, T) is *equicontinuous*, if every point of X is an equicontinuous point for T.
2. A dynamical system (X, T) is *almost equicontinuous*, if the set of equicontinuous points of (X, T) is residual, that is, it contains a countable intersection of dense open sets.
3. A dynamical system (X, T) is *sensitively dependent on initial conditions*, if there exists $\epsilon > 0$ such that for all $x \in X$ and $\delta > 0$, there exists y with $d(x, y) < \delta$ and $d(T^n x, T^n y) \geq \epsilon$ for some $n \geq 0$. We will refer to this property simply as *sensitive*.
4. A dynamical system (X, T) is *transitive*, if there exists at least one transitive point.
5. A dynamical system (X, T) is *mixing*, if for any nonempty open sets $U, V \subseteq X$, there exists $m \in \mathbb{N}$ such that for all $n \geq m$, $T^n(U) \cap V \neq \emptyset$.
6. A dynamical system (X, T) is *positively expansive*, if there exists $\epsilon > 0$ such that for all $x \neq y \in X$, $d(T^n x, T^n y) \geq \epsilon$ for some $n \geq 0$.
7. A dynamical system (X, T) is *chaotic*, if (X, T) is mixing, sensitive and the periodic points are dense in X.

Here we recall the definition of topological entropy, a tool for measuring the complexity of dynamical systems [1]. If a dynamical system has positive topological entropy, then it sometimes implies "chaos".

Let $\mathcal{U}$ be an open cover of X and $H(\mathcal{U}) = \inf \log |\mathcal{V}|$, where the infimum is taken over the set of finite sub-covers $\mathcal{V}$ of $\mathcal{U}$ and $|\mathcal{V}|$ is the number of elements in the set $\mathcal{V}$. Let $\mathcal{U}$ and $\mathcal{V}$ be covers of X. We denote by $\mathcal{U} \vee \mathcal{V}$

the cover made up of all intersections $U \cap V$, where $U \in \mathcal{U}$ and $V \in \mathcal{V}$. The *topological entropy of the cover* $\mathcal{U}$ is defined as

$$h(\mathcal{U}, T) = \lim_{n \to \infty} \frac{1}{n} H\left(\bigvee_{i=0}^{n-1} T^{-i} \mathcal{U} \right).$$

Definition 2 The *topological entropy of* (X, T) is defined by

$$h_{top}(X, T) = \sup_{\mathcal{U}} h(\mathcal{U}, T), \tag{2.1}$$

where the supremum is taken over all finite open covers of X.

The topological entropy of the cover $\mathcal{U}$ and the topological entropy of (X, T) are both non-negative. If two dynamical systems are topologically conjugate then their topological entropies are equal.

2.2. Symbolic dynamics and cellular automata

Let $A = \{0, \dots, k-1\}$ $(k \geq 1)$ be a finite *state* set. A D-dimensional *configuration space* is defined by $A^{\mathbb{Z}^D}$ and each element of $A^{\mathbb{Z}^D}$ is called a *configuration*. For a configuration x and a D-dimensional vector $\xi = (\xi_1, \dots, \xi_D) \in \mathbb{Z}^D$, by x_ξ we mean a state at the coordinate ξ. We define a metric function d_D on $A^{\mathbb{Z}^D}$ for $x, u \in A^{\mathbb{Z}^D}$

$$d_D(x, u) = 2^{-\alpha(x,u)}, \tag{2.2}$$

where $\alpha(x, u) = \min\{\max\{|\xi_1|, \dots, |\xi_D|\} \mid x_\xi \neq u_\xi\}$. Under this metric d_D the space $A^{\mathbb{Z}^D}$ is a compact metric space. The *shift* transformation σ_ζ on $A^{\mathbb{Z}^D}$ is defined by $(\sigma_\zeta x)_\xi = x_{\xi+\zeta}$ for $\zeta \in \mathbb{Z}^D$. In one-dimension the *full shift* σ_e on $A^{\mathbb{Z}}$ is defined by $(\sigma_e y)_l = y_{l+1}$ for $y \in A^{\mathbb{Z}}$. The following statements are well known.

Lemma 1 ([17]) *The full shift* $(A^{\mathbb{Z}}, \sigma_e)$ *is a chaotic dynamical system, that is,* $(A^{\mathbb{Z}}, \sigma_e)$ *is mixing, sensitive and the set of periodic points is dense in* $A^{\mathbb{Z}}$. *The topological entropy of the full shift* $(A^{\mathbb{Z}}, \sigma_e)$ *is*

$$h_{top}(A^{\mathbb{Z}}, \sigma_e) = \log |A|, \tag{2.3}$$

where $|A|$ *is the number of elements in the set* A.

Here we introduce a general definition of a CA.

Definition 3 Let $\xi^{(1)}, \ldots, \xi^{(m)} \in \mathbb{Z}^D$ be distinct vectors for $D \geq 1$. Let T be a shift-commuting, i.e., $T \circ \sigma_\zeta = \sigma_\zeta \circ T$ for $\zeta \in \mathbb{Z}^D$, and continuous map on $A^{\mathbb{Z}^D}$. A discrete dynamical system $(A^{\mathbb{Z}^D}, T)$ is a D-dimensional *cellular automaton* (CA), if T is given by for $x \in A^{\mathbb{Z}^D}$ and each coordinate $\xi \in \mathbb{Z}^D$

$$(Tx)_\xi = f(x_{\xi+\xi^{(1)}}, \ldots, x_{\xi+\xi^{(m)}}), \tag{2.4}$$

where f is a map from A^m to A, called a *local rule.* The *radius* of the CA $(A^{\mathbb{Z}^D}, T)$ is given by $\max\{|\xi_l^{(k)}| \mid 1 \leq k \leq m,\ 1 \leq l \leq D\}$.

The simplest nontrivial CAs are *elementary CAs.* They are one-dimensional CAs with two possible states $A = \{0, 1\}$ and their local rules depend only on the nearest three neighbor states. There exist $2^8 = 256$ elementary CAs, and due to Wolfram, an integer from 0 through 255 is assigned to each elementary CA. A CA is *linear*, if the local rule is linear, i.e.,

$$f(x_{\xi+\xi^{(1)}}, \ldots, x_{\xi+\xi^{(m)}}) = \alpha_1 \cdot x_{\xi+\xi^1} + \cdots + \alpha_m \cdot x_{\xi+\xi^m} \pmod{|A|}$$

for $\alpha_1, \ldots, \alpha_m \in \mathbb{Z}$. A CA is *nonlinear*, if the local rule is not linear.

A *word* is a finite sequence of states from A. For $x \in A^{\mathbb{Z}^D}$ and a finite connected subset of coordinates $S \subset \mathbb{Z}^D$, a *pattern* denoted by $x|_S$ is a D-dimensional generalized word, which is a set of states on S. For a configuration space $A^{\mathbb{Z}^D}$, by $A^{\mathbb{Z}^D}|_S$ we mean a set of all possible patterns on S. A *cylinder set* of a pattern $x|_S$ for $\xi \in \mathbb{Z}^D$ is defined by

$$[x|_S]_\xi = \{x \in A^{\mathbb{Z}^D} \text{ containing } x|_S \text{ beginning at the coordinate given by } \xi\}. \tag{2.5}$$

Every cylinder set is closed and open, and every closed and open set is a finite union of cylinders. A word p for $(A^{\mathbb{Z}}, T)$ is a *blocking word*, if there exist $s, t \in \mathbb{N}$ satisfying $s + t < |p|$ such that if x, u in the cylinder set $[p]_k$ for some $k \in \mathbb{Z}$, then

$$(T^n x)|_{[k+s, k+|p|-t]} = (T^n u)|_{[k+s, k+|p|-t]} \tag{2.6}$$

holds for any $n \geq 0$. Next, we extend the notion of blocking words to higher dimensions. A pattern p of the size $m_1 \times \cdots \times m_D$ for $(A^{\mathbb{Z}^D}, T)$ is a *blocking pattern*, if there exist $s_1, \ldots, s_D, t_1, \ldots, t_D \in \mathbb{N}$ such that for each i, $s_i + t_i < m_i$ and for any $x, u \in [p]_{(k_1,\ldots,k_D)}$ and any $n \geq 0$ we have

$$(T^n x)|_E = (T^n u)|_E, \tag{2.7}$$

where E is a subset of $\mathbb{Z}^D$, $[k_1+s_1, k_1+m_1-t_1]\times\cdots\times[k_D+s_D, k_D+m_D-t_D]$. We also define a stronger notion of blocking: a word p for $(A^{\mathbb{Z}}, T)$ is a *fully blocking word*, if p is a blocking word and $s = t = 0$. For higher dimensional cases, a pattern p of size $m_1 \times \cdots \times m_D$ for $(A^{\mathbb{Z}^D}, T)$ is a *fully blocking pattern*, if p is a blocking pattern and all s_i and t_i are zero.

We consider topological classifications of one-dimensional CAs and multidimensional ($D \geq 2$) CAs (see Figure 1). For one-dimensional CAs Kůrka gave a classification according to the topological behavior [9]. Every one-dimensional CA $(A^{\mathbb{Z}}, T)$ belongs to exactly one of the following four classes; equicontinuous, almost equicontinuous but not equicontinuous, sensitive but not positively expansive, and positively expansive. A one-dimensional almost equicontinuous CA is characterized by the existence of a blocking word [2], while a multidimensional almost equicontinuous CA is characterized by the existence of a D-dimensional hyper-cubic fully blocking pattern [6]. However not all almost-equicontinuous CAs have fully blocking patterns. It is known that there are no multidimensional positively expansive CAs [18], [5]. In particular, every multidimensional linear CA is equicontinuous or sensitive [13]. A linear CA is equicontinuous if and only if it has at least one equicontinuous point.

The following facts are known with respect to the topological entropy of CAs. If a CA is equicontinuous then its topological entropy is zero. The

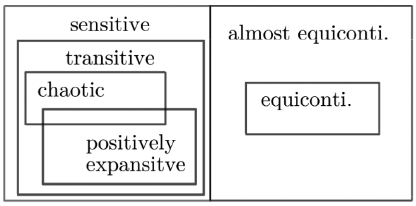

(a) for 1-dim. CAs

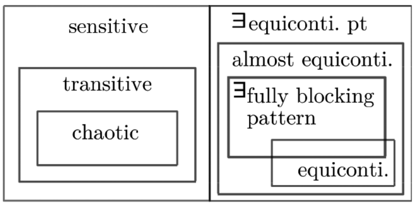

(b) for multidim. CAs

Figure 1. Topological classification of CAs.

topological entropy of a one-dimensional CA is always finite. Positively expansive CAs have nonzero finite topological entropy [4]. If a multidimensional CA is linear, then the topological entropy is either zero or infinity [16], [4]. If a multidimensional CA has a "spaceship" defined in [12], Lakshtanov and Langvagen showed that the topological entropy is infinity [12]. There exists a multidimensional CA with nonzero finite topological entropy [15].

2.3. Inverse ultradiscretization

	cellular automata	max-plus equations	difference equations	differential equations
operations	various ways	$(\max, \pm)$	$(\pm, \times, \div)$	differential operators & $(\pm, \times, \div)$
variables	discrete	discrete	discrete & continuous	continuous

Figure 2. Some forms of equations characterized by the operations and variables.

Inverse ultradiscretization (*IUD*) is a method for deriving PDEs from a CA [11]. The procedure of IUD is the following. First we represent its local rule as an equation represented by operations in a *max-plus algebra* $(\max, \pm)$, which is a semi-ring over $\mathbb{R} \cup \{-\infty\}$ equipped with maximum and addition as the two binary operations. The algebra satisfies the commutative low, the associative law and the distributive law. The unit element for max is $-\infty$ and the identity element for $+$ is 0. The inverse of $a \in \mathbb{R}$ with respect to $+$ is $-a$, as usual, whereas the inverse with respect to max is not defined. Next, we convert the max-plus equation to a continuous equation represented by operations $(\pm, \times, \div)$ by using the identity formula,

$$\max(a, b) = \lim_{\epsilon \to +0} \epsilon \log(e^{a/\epsilon} + e^{b/\epsilon}). \tag{2.8}$$

We introduce a time delay parameter and a propagation speed parameter to control the speed of time or spatial change of solution patterns. We also introduce auxiliary fields which are alternative to cells that the local rule of a given CA depends on (see [11]). Finally we take continuum limits on the parameters and then we obtain a PDE.

There exist some cases that IUD is not success. If we can not represent a given CA as a max-plus equation, then we can not put forward the procedure

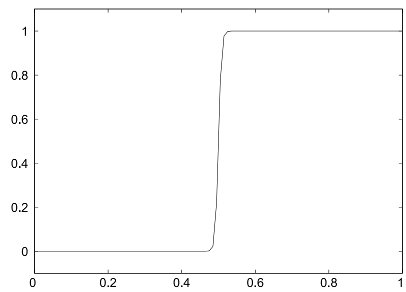

Figure 3. Filter function defined by $\Theta_{\theta,\epsilon}(x) = 1/(1+\exp(-(x-\theta)/\epsilon))$ with $\theta = 0.5$, $\epsilon = 0.004$.

of IUD. Even if we obtain a PDE via IUD, it is a difficult problem to choose the most reasonable PDE which has similar properties to the given CA.

In the procedure of IUD, the obtained difference equation includes a parameter ϵ involved via the identity formula (2.8). For $\epsilon > 0$ the time evolution pattern of the difference equation does not preserve the pattern of a given CA (Figure 4(a)). In order to prevent the lost of the original pattern and obtain the stable time evolution pattern, we give a *filter function* $\Theta_{\theta,\epsilon} : \mathbb{R} \to \mathbb{R}$ for $\epsilon > 0$ and $0 < \theta < 1$. It behaves as $\Theta_{\theta,\epsilon}(x) \cong 0$ for $x < \theta$ and $\Theta_{\theta,\epsilon}(x) \cong 1$ for $x \geq \theta$. As $\epsilon \to +0$, it becomes a step function. In this paper we use the filter function defined by

$$\Theta_{\theta,\epsilon}(x) := \frac{1}{1 + e^{(\theta - x)/\epsilon}}. \tag{2.9}$$

For example, Figure 4 illustrates the pattern of the equation corresponding to Rule 150 without the filter function (a), and with the filter function (b). We can see that without the filter function, the space-time diagram quickly becomes cloudy and disappears in a finite time. By contrast, the

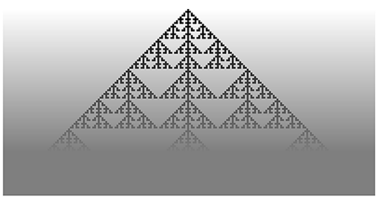

(a) without the filter function

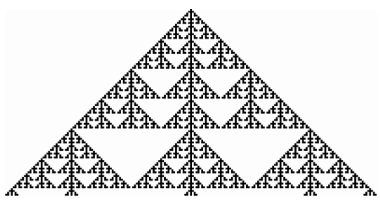

(b) with the filter function

Figure 4. Space-time diagrams of the equation corresponding to Rule 150.

diagram with the filter function is clear and keeps the original pattern for a longer time (numerically, the pattern is kept for an arbitrary long time.)

In Figure 4, 0-cell is represented by a white square and 1-cell is represented by a black square. If a cell has a value in the interval $(0,1)$ we represent the cell by a gray square whose darkness depends on the value.

3. The topological relation between Ulam's CA and Rule 150.

The purpose of this section is to prove that the subsystem of Ulam's CA is topologically conjugate to Rule 150. Ulam's CA is a nonlinear two-dimensional CA, which is a simplified form of a crystalline growth model introduced by Ulam [22]. The model creates the complex patterns (see Figure 5). Rule 150 is an elementary CA and it is known that the CA is one of the nontrivial linear chaotic CA with positive topological entropy. Figure 8 is a space-time diagram of Ulam's CA, which contains a space-time diagram of Rule 150. Moreover we show that the second iteration of Ulam's CA on a subspace is topologically conjugate to Rule 150.

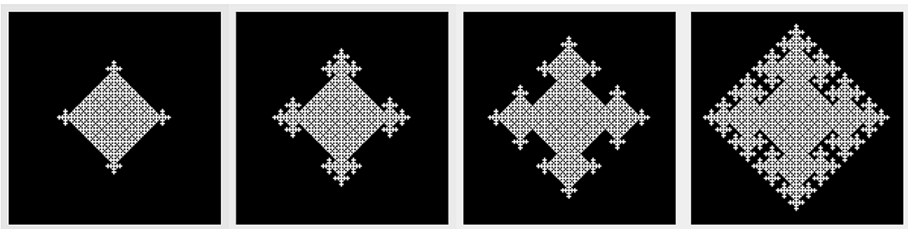

Figure 5. Some patterns created by Ulam's CA $(\mathbf{2}^{\mathbb{Z}^2}, F)$ with the initial configuration consisted of a single site seed

We give the definition of Ulam's CA. Let $\mathbf{2} := \{0,1\}$ be a binary state set, and let $\mathbf{2}^{\mathbb{Z}^2}$ be the two-dimensional configuration space. Ulam's CA $(\mathbf{2}^{\mathbb{Z}^2}, F)$ is defined by a nonlinear local rule;

$$(Fx)_{i,j} = x_{i,j} + x_{i-1,j}x_{i+1,j} + x_{i,j-1}x_{i,j+1} \pmod 2 \tag{3.1}$$

for a configuration $x \in \mathbf{2}^{\mathbb{Z}^2}$.

We need the following lemma to show that Ulam's CA is almost equicontinuous.

Lemma 2 (Gamber [6]) *A D-dimensional CA with radius r is almost* *equicontinuous, if there exists at least one D-dimensional hyper-cubic fully blocking pattern of the size $m \times \cdots \times m$, where $m \geq r$.*

We prove the following proposition by showing the existing of a square fully blocking pattern.

Proposition 1 *Ulam's CA $(\mathbf{2}^{\mathbb{Z}^2}, F)$ is an almost equicontinuous CA.*

Proof. By Lemma 2, it is enough to show that there exists a fully blocking pattern of the size 2×2. We will show that a pattern $\left(\begin{smallmatrix} 0 & 0 \\ 0 & 0 \end{smallmatrix}\right)$ satisfies the requirement. Let x be a configuration in a cylinder set $\left[\begin{smallmatrix} 0 & 0 \\ 0 & 0 \end{smallmatrix}\right]_{(k,l)} \subset \mathbf{2}^{\mathbb{Z}^2}$ for $(k,l) \in \mathbb{Z}^2$, i.e., four states of x are given by $x_{k,l} = x_{k+1,l} = x_{k,l+1} = x_{k+1,l+1} = 0$ (see Figure 6). For the configuration $Fx \in \mathbf{2}^{\mathbb{Z}^2}$ we have

$$\begin{aligned} (Fx)_{k,l} &= 0 + x_{k-1,l} \cdot 0 + x_{k,l-1} \cdot 0 = 0 \\ (Fx)_{k+1,l} &= 0 + 0 \cdot x_{k+2,l} + x_{k+1,l-1} \cdot 0 = 0 \\ (Fx)_{k,l+1} &= 0 + x_{k-1,l+1} \cdot 0 + 0 \cdot x_{k,l+2} = 0 \\ (Fx)_{k+1,l+1} &= 0 + 0 \cdot x_{k+2,l+1} + 0 \cdot x_{k+1,l+2} = 0. \end{aligned} \tag{3.2}$$

Thus, the state of these four cells are kept 0 under the transformation F. Inductively we have for any $n \in \mathbb{N}$, $F^n\left(\left[\begin{smallmatrix} 0 & 0 \\ 0 & 0 \end{smallmatrix}\right]_{(k,l)}\right) \subset \left[\begin{smallmatrix} 0 & 0 \\ 0 & 0 \end{smallmatrix}\right]_{(k,l)}$. Therefore the pattern $\left(\begin{smallmatrix} 0 & 0 \\ 0 & 0 \end{smallmatrix}\right)$ is fully blocking. Hence we conclude that Ulam's CA $(\mathbf{2}^{\mathbb{Z}^2}, F)$ is an almost equicontinuous CA. $\square$

	$x_{k,\,l+2}$	$x_{k+1,\,l+2}$	
$x_{k-1,\,l+1}$	*0*	*0*	$x_{k+2,\,l+1}$
$x_{k-1,\,l}$	*0*	*0*	$x_{k+2,\,l}$
	$x_{k,\,l-1}$	$x_{k+1,\,l-1}$	

Figure 6. Gray cells are $x_{k,l}$, $x_{k+1,l}$, $x_{k,l+1}$ and $x_{k+1,l+1}$.

Next, we consider Rule 150. The figure on the right in Figure 7 is a space-time diagram of Rule 150. There exist eight linear CAs of 256 elementary CAs whose local rules are in table 1. Except for trivial CAs the other four linear elementary CAs, Rule 60, Rule 90, Rule 102 and Rule 150, are either essentially equivalent to Rule 90 or Rule 150. The space-time diagrams of them with single site seeds are fractal self-organizing patterns.

In particular, the space-time diagram of Rule 90 becomes Sierpinski gasket as you take appropriately limit. The nontrivial linear elementary CAs are topologically conjugate to the full shift on 4-symbols [10]. From Lemma 1 we obtain the following statement about topological entropy of them.

Table 1. Local rules of linear elementary CAs.

$y_{l-1}y_ly_{l+1}$	111	110	101	100	011	010	001	000	local rule
Rule 0	0	0	0	0	0	0	0	0	0
Rule 60	0	0	1	1	1	1	0	0	$y_{l-1} + y_l$
Rule 90	0	1	0	1	0	1	1	0	$y_{l-1} + y_{l+1}$
Rule 102	0	1	1	0	0	1	1	0	$y_l + y_{l+1}$
Rule 150	1	0	0	1	0	1	1	0	$y_{l-1} + y_l + y_{l+1}$
Rule 170	1	0	1	0	1	0	1	0	y_{l+1}
Rule 204	1	1	0	0	1	1	0	0	y_l
Rule 240	1	1	1	1	0	0	0	0	y_{l-1}

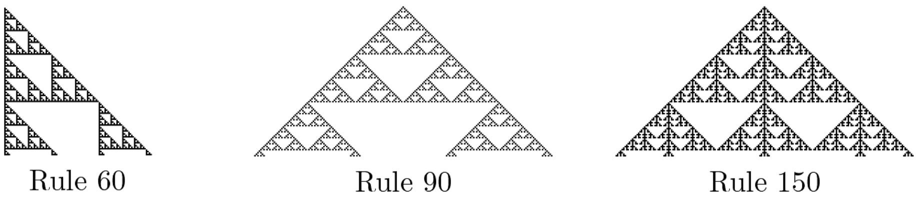

Figure 7. Space-time diagrams with single site seeds.

Proposition 2 ([10]) *Topological entropy of the nontrivial linear elementary CAs are* $2\log 2$*. The CAs are also chaotic, i.e., the CAs are mixing, sensitive and the periodic points are dense in* $\mathbf{2}^{\mathbb{Z}}$*.*

Now we consider the relation between Ulam's CA and Rule 150. The local rule of the linear chaotic CA Rule 150 $(\mathbf{2}^{\mathbb{Z}}, G)$ is given by $(Gy)_l = y_l + y_{l-1} + y_{l+1} \pmod 2$ for $y \in \mathbf{2}^{\mathbb{Z}}$. We show that Ulam's CA has Rule 150 as a subsystem on the particular subspace of $\mathbf{2}^{\mathbb{Z}^2}$. To show that Rule 150 is embedded into Ulam's CA in a nontrivial way, we focus on an unbounded fully blocking pattern as follows.

For a given $K \in \mathbb{N}$ let Ω be a subspace of $\mathbf{2}^{\mathbb{Z}^2}$ defined by

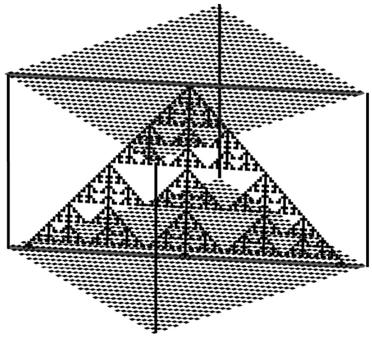

Figure 8. Space-time diagram of Ulam's CA (Ω, F). The fractal-like pattern at the center is equivalent to a space-time diagram of Rule 150 $(\mathbf{2}^{\mathbb{Z}}, G)$.

$$\Omega = \left\{ x \,\middle|\, \begin{array}{ll} x_{i,j} = 1 & \text{if } i+j = K-1,\ K+2 \\ x_{i,j} = 0 & \text{if } i+j = K+3,\ K+4,\ K-2,\ K-3 \\ x_{i,j} \in \mathbf{2} & \text{otherwise.} \end{array} \right\}. \tag{3.3}$$

Let $S = \{(i,j) \in \mathbb{Z}^2 \mid K-3 \le i+j \le K+4\}$ which is a subspace of $\mathbb{Z}^2$. We define a map $\varphi\colon \mathbf{2}^{\mathbb{Z}^2} \to \mathbf{2}^{\mathbb{Z}}$ by

$$y_l := (\varphi x)_l = \begin{cases} x_{k,K-k} & \text{if } l = 2k+1 \\ x_{k,K+1-k} & \text{if } l = 2k \end{cases} \tag{3.4}$$

for $k, l \in \mathbb{Z}$. Each y_l is arranged in a zigzag path in Ω. Then Ulam's CA on the restricted space $\Omega|_S$ and Rule 150 on $\mathbf{2}^{\mathbb{Z}}$ satisfy the following relation.

Theorem 1 *The subsystem* $(\Omega|_S, F)$ *of Ulam's CA and Rule* 150 $(\mathbf{2}^{\mathbb{Z}}, G)$ *are topologically conjugate. That is, the following diagram with a homeomorphism* φ *commutes.*

$$\begin{tikzcd} \Omega|_S \arrow[r, "F"] \arrow[d, "\varphi"'] \arrow[dr, phantom, "\circlearrowleft"] & \Omega|_S \arrow[d, "\varphi"] \\ \mathbf{2}^{\mathbb{Z}} \arrow[r, "G"'] & \mathbf{2}^{\mathbb{Z}}. \end{tikzcd}$$

Proof. Assume without loss of generality that $K = 0$. First we show $F(\Omega) \subset \Omega$. The following patterns (a), (b) are parts of configurations in Ω.

*	1	0	0	*	*	*
*	*	1	0	0	*	*
1	*	*	1	0	0	*
0	1	*	*	1	0	0
0	0	1	*	*	1	0
*	0	0	1	*	*	1
*	*	0	0	1	*	*
*	*	*	0	0	1	*

(a) Gray cells are $x_{i,j}$ with $i+j = -3, -2, -1, 2, 3, 4$.

*	1	0	0	*	*	*
*	*	1	0	0	*	*
1	*	*	1	0	0	*
0	1	*	*	1	0	0
0	0	1	*	*	1	0
*	0	0	1	*	*	1
*	*	0	0	1	*	*
*	*	*	0	0	1	*

(b) Gray cells are $x_{i,j}$ with $i+j = 0, 1$.

Each $*$ at a cell means an arbitrary state, either 0 or 1. We consider a configuration $x \in \Omega$ that fits into the pattern (a). If $i+j=-1$, then the state $x_{i,j} = 1$ and $x_{i-1,j} = x_{i,j-1} = 0$. We have for $x_{i,j}$ with $i+j=-1$,

$$(Fx)_{i,j} = 1 + 0 \cdot x_{i+1,j} + 0 \cdot x_{i,j+1} = 1 = x_{i,j}. \tag{3.5}$$

If $i+j=-2$, we have the states $x_{i,j} = x_{i-1,j} = x_{i,j-1} = 0$ and $x_{i+1,j} = x_{i,j+1} = 1$. Then for $x_{i,j}$ with $i+j=-2$,

$$(Fx)_{i,j} = 0 + 0 \cdot 1 + 0 \cdot 1 = 0 = x_{i,j}. \tag{3.6}$$

If $i+j=-3$, the states $x_{i,j} = x_{i+1,j} = x_{i,j+1} = 0$ and then

$$(Fx)_{i,j} = 0 + x_{i-1,j} \cdot 0 + x_{i,j-1} \cdot 0 = 0 = x_{i,j}. \tag{3.7}$$

In the same way we can obtain $(Fx)_{i,j} = x_{i,j}$ for $x_{i,j}$ with $i+j = 2, 3, 4$. Therefore $x|_S$ is a fully blocking pattern and we have $F(\Omega) \subset \Omega$. Thus, we can consider the subsystem of Ulam's CA on the closed space Ω.

It is sufficient to prove that φ commutes with $(\Omega|_S, F)$ and $(\mathbf{2}^{\mathbb{Z}}, G)$, and φ is a homeomorphism.

We show $\varphi \circ F = G \circ \varphi$. We give a configuration x containing the above pattern (b). If $i+j=0$, then

$$(Fx)_{i,j} = x_{i,j} + 1 \cdot x_{i+1,j} + 1 \cdot x_{i,j+1}, \tag{3.8}$$

because $x_{i-1,j} = x_{i,j-1} = 1$. If $i+j=1$, then

$$(Fx)_{i,j} = x_{i,j} + x_{i-1,j} \cdot 1 + x_{i,j-1} \cdot 1, \tag{3.9}$$

because $x_{i+1,j} = x_{i,j+1} = 1$. Therefore we have for each $l \in \mathbb{Z}$

$$(\varphi \circ F(x))_l = y_l + y_{l-1} + y_{l+1} = (Gy)_l = (G \circ \varphi(x))_l. \tag{3.10}$$

Next we show that the map φ is a homeomorphism between $(\Omega|_S, F)$ and $(\mathbf{2}^{\mathbb{Z}}, G)$. For any $y = (\ldots, y_{l-1}, y_l, y_{l+1}, \ldots) \in \mathbf{2}^{\mathbb{Z}}$, we can represent each state;

$$y_l = (\varphi x)_l = \begin{cases} x_{k,-k} & \text{if } l = 2k+1, \\ x_{k,1-k} & \text{if } l = 2k. \end{cases} \tag{3.11}$$

For $x, u \in \Omega$ if there exist states $x_{i,j}, u_{i,j}$ such that $x_{i,j} \neq u_{i,j}$ with $(i,j) \in S$, then we can take some $k \in \mathbb{Z}$ such that $x_{k,m-k} \neq u_{k,m-k}$ for $m = 0, 1$. Then $(\varphi x)_l = x_{k,m-k} \neq u_{k,m-k} = (\varphi u)_l$. Hence φ is bijective. For the metric functions d_1 on $\mathbf{2}^{\mathbb{Z}}$ and d_2 on $\mathbf{2}^{\mathbb{Z}^2}$ we can obtain immediately $d_2(x,u) \leq d_1(\varphi x, \varphi u)$ for $x, u \in \Omega$. For any $\epsilon > 0$, we can choose $\delta = \sqrt{\epsilon}$ such that if $d_2(x,u) \leq \delta$ then $d_1(\varphi x, \varphi u) \leq \delta^2 = \epsilon$. Therefore both φ and φ^{-1} are continuous. $\square$

Next, we consider a subset of $\mathbb{Z}^2$ defined by $S_m = \{(i,j) \mid i+j = K+m\}$ for $m = 0, 1$ and a map $\varphi_m \colon \Omega|_{S_m} \to \mathbf{2}^{\mathbb{Z}}$ defined by

$$y_l = (\varphi_m x)_l = x_{l,K+m-l} \quad \text{for each } l \in \mathbb{Z}. \tag{3.12}$$

Pictures in Figure 9 are the space-time diagrams of $\varphi_0 \circ F^2$ and $\varphi_1 \circ F^2$. They are analogous to Figure 8 with reason that F is a square root of F^2. Every other row of the diagrams obeys the rule of the CA $(\mathbf{2}^{\mathbb{Z}}, G)$. The figure on the left every odd row and the next even row are identical. The figure on the right there are rows generated by Rule 150 and rows filled with 0-cells appear alternately.

Then on the subspace Ω the second iteration of Ulam's CA $(\mathbf{2}^{\mathbb{Z}^2}, F)$ and Rule 150 keep the following relation.

Proposition 3 *The subsystem $(\Omega|_{S_m}, F^2)$ of the second iteration of Ulam's CA and the elementary CA Rule* 150 $(\mathbf{2}^{\mathbb{Z}}, G)$ *are topologically conjugate for $m = 0, 1$. That is, the following diagram with a homeomorphism φ_m commutes.*

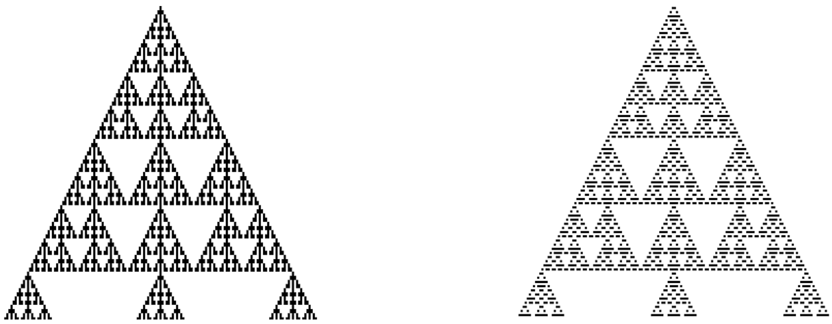

Figure 9. The space-time diagrams of $\varphi_0 \circ F^2$ and $\varphi_1 \circ F^2$.

$$\begin{tikzcd} \Omega|_{S_m} \arrow[r, "F^2"] \arrow[d, "\varphi_m"'] \arrow[dr, phantom, "\circlearrowright"] & \Omega|_{S_m} \arrow[d, "\varphi_m"] \\ \mathbf{2}^{\mathbb{Z}} \arrow[r, "G"'] & \mathbf{2}^{\mathbb{Z}}. \end{tikzcd}$$

Proof. From Theorem 1, $F(\Omega) \subset \Omega$. We consider the second iteration of Rule 150, $(\mathbf{2}^{\mathbb{Z}}, G^2)$. If $y_l = 0$, $(G^2 y)_l = y_{l-2} + y_{l+2} \pmod 2$, while if $y_l = 1$, $(G^2 y)_l = y_{l-2} + y_{l+2} + 1 \pmod 2$. Therefore for all $y \in \mathbf{2}^{\mathbb{Z}}$ we have $(G^2 y)_l = y_{l-2} + y_l + y_{l+2} \pmod 2$. Since $(F^2 x)_{i,j} = x_{i,j} + x_{i-1,j+1} + x_{i+1,j-1}$, for a coordinate $(i,j) \in \mathbb{Z}^2$ with $i + j = m$ we obtain $(\varphi_m \circ F^2(x))_l = y_{l-1} + y_l + y_{l+1}$. Thus $\varphi_m \circ F^2 = G \circ \varphi_m$. We can prove that φ_m is a homeomorphism as is the case with the proof of Theorem 1. $\square$

From Theorem 1 and Proposition 2 we have the result immediately about the topological entropy.

Corollary 1 *Topological entropy of Ulam's CA $(\mathbf{2}^{\mathbb{Z}^2}, F)$ is infinity, because there exist countably many Rule* 150 *embedded into Ulam's CA.*

4. The PDEs associated with Ulam's CA and Rule 150

In this section we derive PDEs from Ulam's CA and Rule 150 via IUD. We make a thorough search of various parameters of PDEs which preserve the self-organizing patterns of given CAs. Finally, we found PDEs as follows.

Lemma 3 *Via IUD, Ulam's CA $(\mathbf{2}^{\mathbb{Z}^2}, F)$ becomes a PDE given in* (4.4)*, which preserves the self-organizing pattern of the CA.*

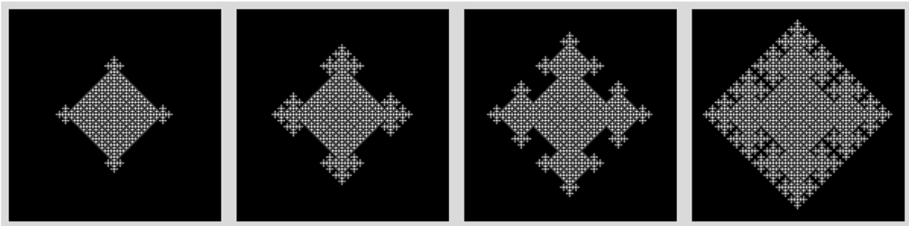

Figure 10. Some patterns created by the PDE corresponding to Ulam's CA with $\epsilon = 0.004$, $\theta = 0.5$, $\Delta t = 0.7$, $\gamma = 1.6$, $\lambda = 0.6$ and the initial configuration $\mathrm{x}(0; e_1, e_2) = 1 - \exp(-(75e_1/0.52)^2) \cdot \exp(-(75e_2/0.52)^2)$ and $\mathrm{u}(0; e_1, e_2) = \mathrm{u}^{(1\pm)}(0; e_1, e_2) = \mathrm{u}^{(2\pm)}(0; e_1, e_2) = 0$.

Proof. Recall that Ulam's CA has the local rule $(Fx)_{i,j} = x_{i,j} + x_{i-1,j}x_{i+1,j} + x_{i,j-1}x_{i,j+1}$ (mod 2). By direct calculation, we can show that this rule is equivalent to the following max-plus equation, provided $x \in \mathbf{2}^{\mathbb{Z}^2}$:

$$
\begin{aligned}
(Fx)_{i,j} = \max\{&x_{i,j}, -\max(-x_{i-1,j}, -x_{i+1,j}), -\max(-x_{i,j-1}, -x_{i,j+1}), \\
&x_{i,j} - \max(-x_{i-1,j}, -x_{i+1,j}) - \max(-x_{i,j-1}, -x_{i,j+1}) - 1\} \\
- \max\{&0, x_{i,j} - \max(-x_{i-1,j}, -x_{i+1,j}) - 1, \\
&- \max(-x_{i-1,j}, -x_{i+1,j}) - \max(-x_{i,j-1}, -x_{i,j+1}) - 1, \\
&- \max(-x_{i,j-1}, -x_{i,j+1}) + x_{i,j} - 1\}.
\end{aligned} \tag{4.1}
$$

To convert this equation into an ordinary differential equation, we replace the discrete variable $x_{i,j} \in \mathbf{2}$ with a continuous one denoted by $\mathrm{x}_{i,j}$ which takes the value in $[0, 1]$. Then we introduce the rescaled variables $\sigma := e^{-(1/\epsilon)}$, $\mathcal{X}_{i,j} := e^{\mathrm{x}_{i,j}/\epsilon}$, $\mathcal{X}_{i\pm} := e^{\mathrm{x}_{i\pm1,j}/\epsilon}$ and $\mathcal{X}_{j\pm} := e^{\mathrm{x}_{i,j\pm1}/\epsilon}$. By using the identity formula (2.8), we obtain the following map $\mathcal{F}_\epsilon : \mathbb{R}^5 \to \mathbb{R}$ with $\epsilon > 0$ for each $(i, j) \in \mathbb{Z}^2$:

$$
\begin{aligned}
&\mathcal{F}_\epsilon(\mathrm{x}_{i,j}, \mathrm{x}_{i\pm1,j}, \mathrm{x}_{i,j\pm1}) \\
&:= \epsilon \log \frac{\mathcal{X}_{i,j} + \dfrac{\mathcal{X}_{i-}\mathcal{X}_{i+}}{\mathcal{X}_{i-} + \mathcal{X}_{i+}} + \dfrac{\mathcal{X}_{j-}\mathcal{X}_{j+}}{\mathcal{X}_{j-} + \mathcal{X}_{j+}} + \dfrac{\sigma\mathcal{X}_{i-}\mathcal{X}_{j-}\mathcal{X}_{i,j}\mathcal{X}_{i+}\mathcal{X}_{j+}}{(\mathcal{X}_{i-} + \mathcal{X}_{i+})(\mathcal{X}_{j-} + \mathcal{X}_{j+})}}{1 + \sigma\left(\dfrac{\mathcal{X}_{i-}\mathcal{X}_{i,j}\mathcal{X}_{i+}}{\mathcal{X}_{i-} + \mathcal{X}_{i+}} + \dfrac{\mathcal{X}_{i-}\mathcal{X}_{i+}}{\mathcal{X}_{i-} + \mathcal{X}_{i+}} \cdot \dfrac{\mathcal{X}_{j-}\mathcal{X}_{j+}}{\mathcal{X}_{j-} + \mathcal{X}_{j+}} + \dfrac{\mathcal{X}_{j-}\mathcal{X}_{i,j}\mathcal{X}_{j+}}{\mathcal{X}_{j-} + \mathcal{X}_{j+}}\right)}.
\end{aligned} \tag{4.2}
$$

By using the filter function $\Theta_{\theta,\epsilon}$ (2.9) and taking the continuum limit, we obtain a differential equation with the parameters $\gamma > 1$ and $\epsilon > 0$:

$$\begin{cases} \dfrac{d}{dt}\mathrm{x}_{i,j}(t) = -\big(\mathrm{x}_{i,j}(t) - \mathcal{F}_\epsilon(\mathrm{u}_{i,j}(t), \mathrm{u}_{i\pm1,j}(t), \mathrm{u}_{i,j\pm1}(t))\big) \\ \dfrac{d}{dt}\mathrm{u}_{i,j}(t) = -\gamma\big(\mathrm{u}_{i,j}(t) - \Theta_{\theta,\epsilon}(\mathrm{x}_{i,j}(t))\big). \end{cases} \tag{4.3}$$

Here the "time-delay" parameter γ denotes the speed ratio of which $\mathrm{x}_{i,j}$ and $\mathrm{u}_{i,j}$ approaches to $\mathcal{F}_\epsilon(\mathrm{u}_{i,j}(t), \mathrm{u}_{i\pm1,j}(t), \mathrm{u}_{i,j\pm1}(t))$ and $\Theta_{\theta,\epsilon}(\mathrm{x}_{i,j}(t))$, respectively. Next, we convert the spatial discrete parameter $(i,j) \in \mathbb{Z}^2$ into a continuous parameter $(e_1, e_2) \in \mathbb{R}^2$. To obtain a well-defined system of PDE, we need to introduce the four auxiliary fields $\mathrm{u}^{(1+)}$, $\mathrm{u}^{(1-)}$, $\mathrm{u}^{(2+)}$ and $\mathrm{u}^{(2-)}$ (see [11]).

	$\mathrm{u}^{(2+)}$	
$\mathrm{u}^{(1-)}$	u	$\mathrm{u}^{(1+)}$
	$\mathrm{u}^{(2-)}$	

Four auxiliary fields are given for each u.

The "propagation speed" parameter $\lambda < 1$ denotes the speed of the spatial change of the patterns. Then we obtain the following PDE:

$$\begin{cases} \dfrac{\partial}{\partial t}\mathrm{x}(t;e_1,e_2) = -\big(\mathrm{x}(t;e_1,e_2) - \mathcal{F}_\epsilon(\mathrm{u}(t;e_1,e_2), \\ \qquad\qquad \mathrm{u}^{(1\pm)}(t;e_1,e_2), \mathrm{u}^{(2\pm)}(t;e_1,e_2))\big) \\ \dfrac{\partial}{\partial t}\mathrm{u}(t;e_1,e_2) = -\gamma\big(\mathrm{u}(t;e_1,e_2) - \Theta_{\theta,\epsilon}\mathrm{x}(t;e_1,e_2)\big) \\ \dfrac{\partial}{\partial t}\mathrm{u}^{(1\pm)}(t;e_1,e_2) \\ \quad = -\gamma\left(\mathrm{u}^{(1\pm)}(t;e_1,e_2) \mp \lambda\dfrac{\partial}{\partial e_1}\mathrm{u}^{(1\pm)}(t;e_1,e_2) - \Theta_{\theta,\epsilon}\mathrm{x}(t;e_1,e_2)\right) \\ \dfrac{\partial}{\partial t}\mathrm{u}^{(2\pm)}(t;e_1,e_2) \\ \quad = -\gamma\left(\mathrm{u}^{(2\pm)}(t;e_1,e_2) \mp \lambda\dfrac{\partial}{\partial e_2}\mathrm{u}^{(2\pm)}(t;e_1,e_2) - \Theta_{\theta,\epsilon}\mathrm{x}(t;e_1,e_2)\right). \end{cases} \tag{4.4}$$

Figure 10 shows the spatial pattern created by (4.4) with the initial configuration $\mathrm{x}(0; e_1, e_2) = 1 - \exp(-(75e_1/0.52)^2) \cdot \exp(-(75e_2/0.52)^2)$ and $\mathrm{u}(0; e_1, e_2) = \mathrm{u}^{(1\pm)}(0; e_1, e_2) = \mathrm{u}^{(2\pm)}(0; e_1, e_2) = 0$. The figure enjoys an apparent similarity to the pattern created by Ulam's CA. $\square$

Next we apply IUD to Rule 150 $(\mathbf{2}^{\mathbb{Z}}, G)$. Let $\hat{\gamma} > 1$ be the time delay parameter and $\hat{\lambda} < 1$ be the propagation speed parameter, as in the case of Ulam's CA.

Lemma 4 *Via IUD, Rule* 150 $(\mathbf{2}^{\mathbb{Z}}, G)$ *becomes a PDE given in* (4.8)*, which preserves the self-organizing pattern of the CA.*

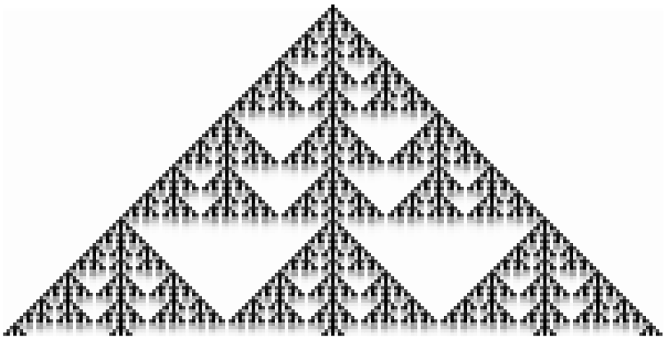

Figure 11. Evolution of the PDE for $\mathcal{G}_{\hat{\epsilon}}$ with $\hat{\epsilon} = 0.005$, $\theta = 0.4$, $\Delta t = 0.7$, $\hat{\gamma} = 1.6$, $\hat{\lambda} = 0.9$ and the initial condition $\mathrm{y}(0; s) = \exp(-(75s/0.52)^2)$ and $\mathrm{p}(0; s) = \mathrm{p}^{(\pm)}(0; s) = 0$.

Proof. We recall the elementary CA Rule 150 has the local rule $(Gy)_l = y_l + y_{l-1} + y_{l+1} \pmod 2$ for $y \in \mathbf{2}^{\mathbb{Z}}$. By direct calculation, we can show that this rule is equivalent to the following max-plus equation:

$$
\begin{aligned}
(Gy)_l = \max\big\{ & y_{l-1} - \max(y_{l-1} - 1, 0), y_l, y_{l+1} - \max(y_{l+1} - 1, 0), \\
& y_{l-1} - \max(y_{l-1} - 1, 0) + y_l + y_{l+1} - \max(y_{l+1} - 1, 0) - 1 \big\} \\
- \max\big\{ & 0, y_{l-1} - \max(y_{l-1} - 1, 0) + y_l - 1, \\
& y_l + y_{l+1} - \max(y_{l+1} - 1, 0) - 1, \\
& y_{l+1} - \max(y_{l+1} - 1, 0) + y_{l+1} - \max(y_{l+1} - 1, 0) - 1 \big\}.
\end{aligned}
\tag{4.5}
$$

To convert this equation into an ordinary differential equation, we replace the discrete variable $y_l \in \mathbf{2}$ with a continuous one denoted by y_l which takes the value in $[0,1]$. Then we introduce the rescaled variables $\mathcal{Y}_l := e^{\mathrm{y}_l/\hat{\epsilon}}$, $\mathcal{Y}_{l\pm1} := e^{\mathrm{y}_{l\pm1}/\hat{\epsilon}}$ and $\hat{\sigma} := e^{-1/\hat{\epsilon}}$. By using the identity formula (2.8), the map $\mathcal{G}_{\hat{\epsilon}} : \mathbb{R}^3 \to \mathbb{R}$ with $\hat{\epsilon} > 0$ is given by for each $l \in \mathbb{Z}$:

$$\begin{aligned}
&\mathcal{G}_{\hat{\epsilon}}(\mathrm{y}_l, \mathrm{y}_{l\pm1}) \\
&:= \hat{\epsilon} \log \frac{\dfrac{\mathcal{Y}_{l-1}}{\hat{\sigma}\mathcal{Y}_{l-1}+1} + \mathcal{Y}_l + \dfrac{\mathcal{Y}_{l+1}}{\hat{\sigma}\mathcal{Y}_{l+1}+1} + \dfrac{\hat{\sigma}\mathcal{Y}_{l-1}\mathcal{Y}_l\mathcal{Y}_{l+1}}{(\hat{\sigma}\mathcal{Y}_{l-1}+1)(\hat{\sigma}\mathcal{Y}_{l+1}+1)}}{1+\hat{\sigma}\left(\dfrac{\mathcal{Y}_{l-1}\mathcal{Y}_l}{\hat{\sigma}\mathcal{Y}_{l-1}+1} + \dfrac{\mathcal{Y}_l\mathcal{Y}_{l+1}}{\hat{\sigma}\mathcal{Y}_{l+1}+1} + \dfrac{\mathcal{Y}_{l+1}\mathcal{Y}_{l-1}}{(\hat{\sigma}\mathcal{Y}_{l+1}+1)(\hat{\sigma}\mathcal{Y}_{l-1}+1)}\right)}.
\end{aligned} \tag{4.6}$$

The filter function $\Theta_{\theta,\hat{\epsilon}}$ (2.9) is adopted and we take the continuum limit. Then we obtain a differential equation with the time delay parameter $\hat{\gamma} > 1$,

$$\begin{cases} \dfrac{d}{dt}\mathrm{y}_l(t) = -\big(\mathrm{y}_l(t) - \mathcal{G}_{\hat{\epsilon}}(\mathrm{p}_l(t), \mathrm{p}_{l\pm1}(t))\big) \\ \dfrac{d}{dt}\mathrm{p}_l(t) = -\hat{\gamma}\big(\mathrm{p}_l(t) - \Theta_{\theta,\hat{\epsilon}}(\mathrm{y}_l(t))\big). \end{cases} \tag{4.7}$$

We convert the spatial discrete parameter $l \in \mathbb{Z}$ into a continuous parameter $s \in \mathbb{R}$. To obtain a well-defined system of PDE, we need to introduce the auxiliary fields $p^{(+)}(t;s)$, $p^{(-)}(t;s)$ and the propagation speed $\hat{\lambda} < 1$ (see [11]). The we obtain the following PDE:

$$\begin{cases} \dfrac{\partial}{\partial t}\mathrm{y}(t;s) = -\big(\mathrm{y}(t;s) - \mathcal{G}_{\hat{\epsilon}}(\mathrm{p}(t;s), \mathrm{p}^{(+)}(t;s), \mathrm{p}^{(-)}(t;s))\big) \\ \dfrac{\partial}{\partial t}\mathrm{p}(t;s) = -\hat{\gamma}\big(\mathrm{p}(t;s) - \Theta_{\theta,\hat{\epsilon}}(\mathrm{y}(t;s))\big) \\ \dfrac{\partial}{\partial t}\mathrm{p}^{(+)}(t;s) = -\hat{\gamma}\left(\mathrm{p}^{(+)}(t;s) - \hat{\lambda}\dfrac{\partial}{\partial s}\mathrm{p}^{(+)}(t;s) - \Theta_{\theta,\hat{\epsilon}}(\mathrm{y}(t;s))\right) \\ \dfrac{\partial}{\partial t}\mathrm{p}^{(-)}(t;s) = -\hat{\gamma}\left(\mathrm{p}^{(-)}(t;s) + \hat{\lambda}\dfrac{\partial}{\partial s}\mathrm{p}^{(-)}(t;s) - \Theta_{\theta,\hat{\epsilon}}(\mathrm{y}(t;s))\right). \end{cases} \tag{4.8}$$

Figure 11 shows the spatial pattern created by (4.8) with the initial configuration $\mathrm{y}(0;s) = \exp(-(75s/0.52)^2)$ and $\mathrm{p}(0;s) = 0$. The figure enjoys an apparent similarity to the pattern created by Rule 150. □

Finally, we consider the relation between the PDE (4.4) associated with Ulam's CA and the PDE (4.8) associated with Rule 150.

Let $\hat{S} := \{(e_1, e_2) \in \mathbb{R}^2$ satisfying $e_2 - e_1 = 3/2\} \subset \mathbb{R}^2$. We numerically solve the PDE (4.4) with the following initial configuration: $\mathrm{x}(e_1, e_2) = \max(h_1(e_1, e_2), h_2(e_1, e_2))$ and $\mathrm{u}(0; e_1, e_2) = \mathrm{u}^{(1\pm)}(0; e_1, e_2) = \mathrm{u}^{(2\pm)}(0; e_1, e_2) = 0$, where the maps $h_1 : \mathbb{R}^2 \to \mathbb{R}$ and $h_2 : \mathbb{R}^2 \to \mathbb{R}$ are defined by

$$h_1(e_1, e_2) = \begin{cases} \exp(-((75e_1 + 75e_2 + 1)/0.52)^2) & \text{if } e_1 + e_2 \leq 0 \\ \exp(-((75e_1 + 75e_2 - 1)/0.52)^2) & \text{if } e_1 + e_2 \geq 0, \end{cases} \tag{4.9}$$

$$h_2(e_1, e_2) = \exp(-(75e_1/0.52)^2) \cdot \exp(-(75e_2/0.52)^2). \tag{4.10}$$

The map h_1 corresponds to the condition of a configuration being in Ω (3.3). The map h_2 gives a single site seed in $\hat{S}$. We restrict the solution on $\hat{S}$ and then obtain Figure 12. We compare Figure 12 with Figure 11, the evolution pattern of (4.8); two figures are definitely similar to each other. This observation can be summarized as follows:

Theorem 2 *The solution on $\hat{S}$ of the evolution pattern of the PDE* (4.4) *associated with Ulam's CA and the evolution pattern of the PDE* (4.8) *associated with Rule* 150 *are similar in the sense of* [11].

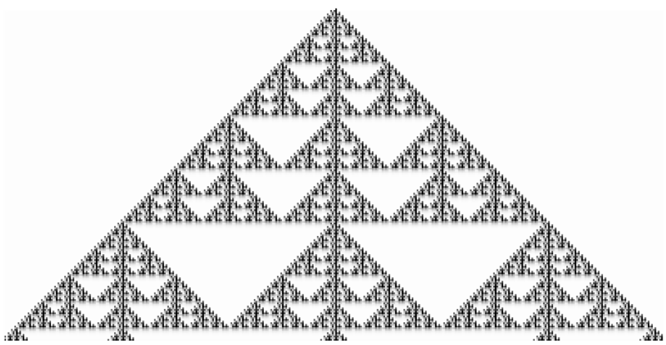

Figure 12. The solution on $\hat{S}$ of the PDE for $\mathcal{F}_\epsilon$ with $\epsilon = 0.004$, $\theta = 0.5$, $\Delta t = 0.7$, $\gamma = 1.6$, $\lambda = 0.8$ with the initial condition $\mathrm{x}(0; e_1, e_2) = \max(h_1(e_1, e_2), h_2(e_1, e_2))$ and $\mathrm{u}(0; e_1, e_2) = \mathrm{u}^{(1\pm)}(0; e_1, e_2) = \mathrm{u}^{(2\pm)}(0; e_1, e_2) = 0$.

5. Conclusion

In this paper we considered the relation between CAs and PDEs in Figure 13.

We showed that the elementary CA Rule 150 is embedded into Ulam's CA. An interesting new phenomenon is shown by the existence of the unbounded fully blocking pattern. The pattern divides the configuration space of Ulam's CA into a one-dimensional configuration space and the other spaces. However, it is not likely that the same method can immediately be applied to find another non-trivial example; it is difficult to find a fully blocking pattern that separates a one-dimensional invariant space.

Via IUD, we derived PDEs from Ulam's CA and Rule 150. We showed that the numerical evolution patterns of these PDEs are similar to each other. This successful example is an essential first step in understanding the relation between CAs and PDEs.

As far as the author knows, there exist only a few results on IUD [11], [19]. The reason might be that the procedure of IUD has some subtlety and there is no canonical way to determine the best PDE. To overcome this difficulty, it would be useful to define an index that measures the difference between the patterns of obtained PDEs and that of the original CA.

$$\begin{tikzcd}
\text{Ulam's CA} \arrow[r, "\text{Th.1}"] \arrow[d, "\text{Lem.3}"] & \text{Rule150} \arrow[d, "\text{Lem.4}"] \\
\text{PDE for } \mathcal{F}_\epsilon \arrow[r, "\text{Th.2}"] & \text{PDE for } \mathcal{G}_{\hat{\epsilon}}
\end{tikzcd}$$

Figure 13. Outline of the relation between the CAs and their PDEs.

References

[1] Adler R. L., Konheim A. G. and McAndrew M. H., *Topological entropy.* Trans. Amer. Math. Soc. **114** (1965), 309–319.

[2] Blanchard F. and Tisseur P., *Some properties of cellular automata with equicontinuity points.* Ann. Inst. H. Poincaré Probab. Statist. **36**(5) (2000), 569–582.

[3] Blanchard F., Køcircurka P. and Maass A., *Topological and measure-theoretic properties of one-dimensional cellular automata.* Phys. D **103**(1–4) (1997), 86–99, Lattice dynamics (Paris, 1995).

[4] D'amico M., Manzini G. and Margara L., *On computing the entropy of cellular automata*. Theoret. Comput. Sci. **290**(3) (2003), 1629–1646.

[5] Finelli M., Manzini G. and Margara L., *Lyapunov exponents versus expansivity and sensitivity in cellular automata*. J. Complexity **14**(2) (1998), 210–233.

[6] Gamber E., *Equicontinuity properties of D-dimensional cellular automata*. Topology Proc. **30**(1) (2006), 197–222. Spring Topology and Dynamical Systems Conference.

[7] Grosse-Erdmann K.-G. and Peris Manguillot A., *Linear chaos*. Universitext. Springer, London, 2011.

[8] Hedlund G. A., *Endormorphisms and automorphisms of the shift dynamical system*. Math. Systems Theory **3** (1969), 320–375.

[9] Køcircurka P., *Languages, equicontinuity and attractors in cellular automata*. Ergodic Theory Dynam. Systems **17**(2) (1997), 417–433.

[10] Køcircurka P., *Topological and symbolic dynamics*, volume 11 of *Cours Spécialisés [Specialized Courses]*. Société Mathématique de France, Paris, 2003.

[11] Kunishima W., Nishiyama A., Tanaka H. and Tokihiro T., *Differential equations for creating complex cellular automaton patterns*. J. Phys. Soc. Japan, **73**(8) (2004), 2033–2036.

[12] Lakshtanov E. L. and Langvagen E. S., *A criterion for the infinity of the topological entropy of multidimensional cellular automata*. Problemy Peredachi Informatsii **40**(2) (2004), 70–72.

[13] Manzini G. and Margara L., *A complete and efficiently computable topological classification of D-dimensional linear cellular automata over Z_m*. In *Automata, languages and programming* (*Bologna,* 1997), volume 1256 of *Lecture Notes in Comput. Sci.*, pages 794–804. Springer, Berlin, 1997.

[14] Martin G., *Mathematical games*. Scientific American **223** (1970), 120–123.

[15] Meyerovitch T., *Finite entropy for multidimensional cellular automata*. Ergodic Theory Dynam. Systems **28**(4) (2008), 1243–1260.

[16] Morris G. and Ward T., *Entropy bounds for endomorphisms commuting with K actions*. Israel J. Math. **106** (1998), 1–11.

[17] Robinson C., *Dynamical systems*. Studies in Advanced Mathematics. CRC Press, Boca Raton, FL, 1995. Stability, symbolic dynamics, and chaos.

[18] Shereshevsky M. A., *Expansiveness, entropy and polynomial growth for groups acting on subshifts by automorphisms*. Indag. Math. (N.S.), **4**(2) (1993), 203–210.

[19] Tanaka H., Nishiyama A. and Tokihiro T., *Cellular automaton no gyakuchōrisanka to bz hannō heno ōyō*. In *Sūrikaisekikenkyūsho Kōkyūroku*, 1473,

From Soliton Theory to a Mathematics of Integrable Systems: "New Perspectives" (Japanese) (Kyoto, 2006), 15–20, 2006.

[20] Tokihiro T., Takahashi D., Matsukidaira J. and Satsuma J., *From soliton equations to integrable cellular automata through a limiting procedure*. Phys. Rev. Lett. **76** (1996), 3247–3250.

[21] Ulam S., *Random processes and transformations*. In *Proceedings of the International Congress of Mathematicians*, **2**, Cambridge, Mass., 1950, pp. 264–275, Providence, R. I., 1952. Amer. Math. Soc.

[22] Ulam S., *On some mathematical problems connected with patterns of growth of figures*. the Proceedings of Symposia in Applied Mathematics **14** (1962), 215–224.

[23] von Neumann J., *The general and logical theory of automata*. In *Cerebral Mechanisms in Behavior*. The Hixon Symposium, pp. 1–31; discussion, pp. 32–41. John Wiley & Sons Inc., New York, N. Y., 1951.

[24] Wolfram S., *Statistical mechanics of cellular automata*. Rev. Modern Phys. **55**(3) (1983), 601–644.

[25] Wolfram S., *Twenty problems in the theory of cellular automata*. Phys. Scripta, **T9** (Vol. T9) (1985), 170–183. Physics of chaos and related problems (Gräftåvallen, 1984).

Department of Mathematics
Hokkaido University
Kita-10, Nishi-8, Kita-ku
Sapporo 060-0810, Japan
E-mail: aka@math.sci.hokudai.ac.jp